1   **Sex-specific age-related changes in glymphatic function assessed by resting-state functional**

2   **magnetic resonance imaging**

3

4   Feng Han[1], Xufu Liu[1], Yifan Yang[1], Xiao Liu[1,2] *

5   **Affiliations:**

6   [1] Department of Biomedical Engineering, The Pennsylvania State University, PA, USA;

7   [2] Institute for Computational and Data Sciences, The Pennsylvania State University, PA, USA

8   *Correspondence to: xxl213@psu.edu

9

Summary

The glymphatic system that clears out brain wastes, such as amyloid-β (Aβ) and tau, through cerebrospinal fluid (CSF) flow may play an important role in aging and dementias. However, a lack of non-invasive tools to assess the glymphatic function in humans hindered the understanding of the glymphatic changes in healthy aging. The global infra-slow (<0.1 Hz) brain activity measured by the global mean resting-state fMRI signal (gBOLD) was recently found to be coupled by large CSF movements. This coupling has been used to measure the glymphatic process and found to correlate with various pathologies of Alzheimer's disease (AD), including Aβ pathology. Using resting-state fMRI data from a large group of 719 healthy aging participants, we examined the sex-specific changes of the gBOLD-CSF coupling, as a measure of glymphatic function, over a wide age range between 36-100 years old. We found that this coupling index remains stable before around age 55 and then starts to decline afterward, particularly in females. Menopause may contribute to the accelerated decline in females.

Introduction

30

31

32   Aging is the leading risk factor for cognitive decline and neurodegenerative disorders that are often

33   associated with excessive accumulation of misfolded proteins, including the amyloid-β and tau, in

34   the brain (Hou et al., 2019; Mawuenyega et al., 2010; Peng et al., 2016). Recent studies suggested

35   the aggregation of toxic proteins could be partly attributed to impaired glymphatic clearance at

36   advancing ages (Benveniste et al., 2019; Boland et al., 2018; Jessen et al., 2015). The glymphatic

37   system, as "glia-lymphatic system", constitutes a pathway for brain waste clearance in the central

38   nervous system (Iliff et al., 2012; Jessen et al., 2015). In this clearance pathway, cerebrospinal

39   fluid (CSF) moves from the periarterial space, facilitated by aquaporin-4 (AQP4) channels in

40   astroglial endfeet, into the interstitial space to wash out interstitial solutes, including Aβ and tau,

41   into the perivenous space surrounding deep-draining veins (Jessen et al., 2015; Tarasoff-Conway

42   et al., 2015). The paravascular CSF recirculation and interstitial solute efflux have been found to

43   decrease in aged mice due to widespread loss of perivascular AQP4 polarization and reduced

44   pulsatility of intracortical arterioles (Kress et al., 2014). In humans, the clearance along the

45   glymphatic pathway and downstream meningeal lymphatic vessels, measured by contrast-agent

46   MRI, decreased and delayed in older patients as compared with younger ones (Zhou et al., 2020).

47   However, the invasive nature of these imaging tools has hindered a large-scale study of glymphatic

48   function in healthy aging subjects. As a result, it remains unclear how the glymphatic function

49   changes in aging, which is vital to understanding the mechanisms of age-related neurodegenerative

50   disorders and cognitive decline.

51

52   Global infra-slow (< 0.1 Hz) brain activity measured by resting-state fMRI (rsfMRI) was recently

53   linked to the glymphatic function (Kiviniemi et al., 2016) and used to quantify its changes in

54   Alzheimer's disease (AD) (Han et al., 2021b) and Parkinson's disease (PD) patients (Han et al.,

55   2021a). Increasing evidence suggested the brain exhibits highly structured, brain-wide infra-slow

56   (< 0.1 Hz) activity during the resting state (Gu et al., 2021; Liu et al., 2021; Raut et al., 2021;

57   Thompson et al., 2014). This global brain activity is evident in neural signals of distinct scales,

58   ranging from single neuron recordings to whole-brain fMRI, and closely related to transient

59   arousal modulations (Gu et al., 2021; Liu et al., 2021). The fMRI measure of this activity, i.e., the

60   global mean rsfMRI blood-oxygenation-level-dependent (gBOLD) signal, is coupled by large CSF

61   movements (Fultz et al., 2019) and astroglial calcium waves (Wang et al., 2018), suggesting its

62   potential link to the glymphatic function. The gBOLD is greatly enhanced during sleep (Fukunaga

63   et al., 2006; Larson-Prior et al., 2009; Olbrich et al., 2009), in accordance with the sleep-enhanced

64   nature of the glymphatic function (Xie et al., 2013). In contrast, arterial and respiratory pulsations,

65   which had been traditionally regarded as the main glymphatic drivers (Iliff et al., 2013; Yamada

66   et al., 2013), actually lack of this attribute with the decreased amplitude during sleep (Boudreau et

67   al., 2013; Douglas et al., 1982; Snyder et al., 1964). For all these reasons, the strength of gBOLD-

68   CSF coupling has been proposed as a surrogate measure of the glymphatic function and found to

69   correlate with various AD pathologies and cognitive decline in PD (Han et al., 2021b, 2021a).

70   Recently, the disengagement of gBOLD from the default mode network (DMN) regions were

71   found to account for early, preferential Aβ accumulation in these higher-order brain areas in the

72   early stage of Aβ pathology (Han et al., 2022). In these early studies, the gBOLD-CSF coupling

73   also was found to correlate significantly with age and sex (Han et al., 2021b, 2021a), but the related

74   findings were limited by narrow age ranges and complicated by the inclusion of patient data.

75

76   The fMRI-based glymphatic measurement, together with the widely available rsfMRI data,

77   provides us a unique opportunity to study the change of the glymphatic function over a wider age

78   range and in a larger population of healthy aging subjects. In this study, we used rsfMRI data of

79   719 healthy aging subjects in the Human Connectome Project Aging (HCP-A) (Harms et al., 2018)

80   to study the age-related changes in glymphatic function in a sex-specific way. We found that the

81   fMRI-based glymphatic measure remained relatively stable within the range of age 36-54 and then

82   started to decrease around age mid-50s. Compared with males, females showed a larger and more

83   abrupt decline of the glymphatic function at this transitioning point. In addition, menopause may

84   lead to an accelerated glymphatic decline in females.

85

86   **Results**

87

88   **Nonlinear age trajectory of the gBOLD-CSF coupling**

89

90   We used rsfMRI data of 719 healthy subjects (403 females) from the HCP-A project with age

91   ranging from 36 to 100. Following previous procedures (Fultz et al., 2019; Han et al., 2021b,

92   2021a), we obtained the whole-brain gBOLD signal from the gray matter regions and the bottom-

93   slice CSF signal around the bottom of the cerebellum to measure CSF movements via MR inflow

94   effects (Fultz et al., 2019; Gao et al., 1996; Gao and Liu, 2012) (**Fig. S1A** and **S1B**). Consistent

95   with the previous studies, the averaged cross-correlation function of the two signals displayed a

96   biphasic pattern with a negative peak ($r = -0.33$) at the +3.2 sec lag (**Fig. S1C**). The gBOLD-CSF

97   correlation at this +3.2 sec time lag was then computed for individual subjects to quantify their

98   coupling and thus the glymphatic function. The gBOLD-CSF coupling was then averaged within

99   10 equal-size groups of subjects at different ages, and the resulting age-related trend displayed a

100   clear non-linear trajectory: it remains relatively stable between ages 36 to 54 and then begins to

101   decline at around 55 years old (i.e., yrs) (**Fig. 1A**). We then divided the entire cohort into younger

102   and older groups according to the age boundary (53.9 yrs) between the fourth and fifth groups,

103   which had the largest drop among pairs of consecutive groups. The gBOLD-CSF coupling is not

104   correlated ($r = -3.7\times10^{-3}$, $p = 0.95$) with age in the younger group whereas this correlation is

105   significant ($r = 0.14$, $p = 3.9\times10^{-3}$) in the older group (**Fig. 1B**).

106

107   We examined potential factors mediating this age-coupling association. Neither the coupling index

108   nor age was significantly correlated with the total Pittsburgh Sleep Quality Index (PSQI) score,

109   but they were similarly correlated with a few PSQI items, including sleep medication, trouble

110   sleeping, and sleep hours. Nevertheless, the age-related changes in the gBOLD-CSF coupling

111   remain largely unchanged with adjusting for these sleep-related measurements (**Fig. 2**). Likewise,

112   the age trajectory of the gBOLD-CSF remained similar with controlling for other non-sleep factors,

113   including the head motion assessed by mean framewise displacement (FD) (**Fig. S2**), the brain

114   volume (**Fig. S3**), and the CSF volume (mainly from the ventricles) (**Fig. S4**), even though these

115   factors showed a significant dependence on age (all $p < 3.9\times10^{-7}$ for linear regression).

116

117   **Sex-specific differences in age-related changes**

118

119   The gBOLD–CSF coupling is different between females and males. The mean gBOLD-CSF

120   strength is significantly ($p = 7.9\times10^{-6}$, two-sample t-test) weaker in females than males (**Fig. 3A**),

121   consistent with the previous finding in an AD cohort (Han et al., 2021b). The age trajectories of

122   the coupling index are different for the two groups. The gBOLD–CSF coupling decreases more

123   evidently and abruptly with aging in the females, particularly around 55 yrs, whereas the males

124   showed a more gradual and steady age-related changes (**Fig. 3B**).

125

126   We further tested whether and how the gBOLD-CSF coupling is affected by menopause, which

127   often occurs before age 55. This analysis was focused on the age range of 36-55, which includes

128   both post-menopause and other females. The menopause status had no significant effects on the

129   gBOLD-CSF coupling strength for two subgroups of subjects of similar ages (both $p > 0.13$; two

130   sample t-test). However, it showed a marginally significant ($p = 0.061$) interaction with age on the

131   coupling strength. Consistent with this result, the gBOLD-CSF coupling in the postmenopausal

132   females appeared to decline earlier in the age mid-40s (**Fig. 3C**), making the drop around age 55

133   less abrupt and significant ($p = 0.058$). The result suggests the potential effect of the menopause

134   to accelerate the decline of the fMRI-based glymphatic measure.

135

136   **Discussion**

137

138   Here we study the sex-specific age-related change in the glymphatic function in a large healthy

139   aging population based on the gBOLD-CSF coupling measured by rsfMRI. We showed that the

140   gBOLD-CSF coupling changes with age in a non-linear way: it remains relatively stable from 36

141   yrs to 54 yrs and then begins to decrease afterwards. Importantly, the decrease at age mid-50s is

142   larger and more abrupt in females than in males.

143

144   Converging evidence has suggested a link between the glymphatic function and the resting-state

145   global brain activity, often measured by the gBOLD signal of rsfMRI. The gBOLD, once regarded

146   as noise, measured a brain-wide, low-frequency (< 0.1 Hz) activity linked to transient arousal

147   modulations, which also has been observed in monkey electrocorticography (ECoG) (Liu et al.,

148   2015, 2018) and mice spiking data as highly structured patterns (Liu et al., 2021). The low-

149   frequency rsfMRI signals were first linked to the glymphatic function due to their potential link to

150   CSF dynamics and vasomotor waves (Kiviniemi et al., 2016). It was found later that it is the global

151   component of rsfMRI, i.e., gBOLD, that is coupled to CSF movements in a sleep-dependent way

152   (Fukunaga et al., 2006; Fultz et al., 2019; Helakari et al., 2022; Larson-Prior et al., 2009; Olbrich

153   et al., 2009). The sleep dependency makes it more suitable for driving the sleep-dependent

154   glymphatic clearance (Holth et al., 2019; Xie et al., 2013), as compared with the cardiac and

155   respiratory pulsations that are actually suppressed during sleep (Baust and Bohnert, 1969;

156   Boudreau et al., 2013; Douglas et al., 1982; Guazzi and Zanchetti, 1965; Snyder et al., 1964).

157   Nevertheless, the gBOLD is not independent from these physiological drivers but shows strong

158   correlations with the low-frequency modulation of cardiac and respiratory functions (Birn et al.,

159   2006; Chang et al., 2009; Gu et al., 2020; Özbay et al., 2019, 2018; Power et al., 2018). Consistent

160   with these human findings of strong low-frequency physiological modulation, a recent mice study

161   demonstrated very strong arterial constrictions/dilations during sleep in the same frequency range

162   (<0.1 Hz) (Turner et al., 2020). Such low-frequency vessel modulations were coupled by pupil

163   size changes suggestive of transient arousal modulations (Turner et al., 2022), similar to the global

164   brain activity measured by gBOLD (Liu et al., 2021, 2018; Pais-Roldán et al., 2020; Turchi et al.,

165   2018). Animal research also suggested that the gBOLD is coupled by large calcium signals of

166   astrocytes (Pais-Roldán et al., 2020), and the AQP4 channels on the endfeet of these cells are a

8

167   key player of the glymphatic system (Iliff et al., 2012; Jessen et al., 2015). To date, the key

168   evidence linking the gBOLD to the glymphatic function came from a human study showing that

169   the gBOLD is coupled to large CSF movements (Fultz et al., 2019). Based on this, the gBOLD-

170   CSF coupling was used to quantify glymphatic function and found correlated with various

171   pathologies of AD and cognitive decline in PD (Han et al., 2021b, 2021a). The preferential

172   reduction of gBOLD signal in the higher-order default mode network was found to account for

173   early, preferential β-amyloid accumulations in the same regions at the early stage of AD (Han et

174   al., 2022). All these findings established the foundation for using the gBOLD-CSF coupling to

175   measure the glymphatic function. But a direct proof of their relationship would need future

176   experiments capable of recording brain signals across distinct spatial and temporal scales. It is also

177   worth noting that the debate is ongoing regarding specific components of glymphatic theory, e.g.,

178   the convective flow in the interstitial space and the involvement of AQP4 channels in the process

179   (Abbott et al., 2018; Hladky and Barrand, 2022). Nevertheless, a consensus view is reached

180   regarding the existence of periarterial CSF flow (Mestre et al., 2018) and its role in waste clearance

181   (van Veluw et al., 2020), which is more related to the gBOLD-CSF coupling in the present study.

182

183   Brain aging affects the glymphatic function. The CSF inflow of larger tracers or macromoleculars

184   decreased up to 85% in old wild-type mice as compared to young counterpart (Da Mesquita et al.,

185   2018; Nedergaard and Goldman, 2020). The decreased glymphatic flow in aged mice has been

186   partly attributed to dysregulation of astroglial water transport due to the widespread loss of AQP4

187   polarization (Kress et al., 2014), the decline of CSF pressure (Fleischman et al., 2012), and the

188   changes of CSF secretion and protein content (Chen et al., 2009). Arterial wall stiffening and

189   associated reduction of arterial pulsatility (Zieman et al., 2005) may also account for age-related

190   glymphatic reduction (Iliff et al., 2013). Human studies of glymphatic function remain sparse (Eide

191   et al., 2018; Zhou et al., 2020). Previous studies using the gBOLD-CSF coupling found a consistent

192   association between the age and glymphatic function, but only in patients of relatively old ages

193   (Han et al., 2021a, 2021b). A retrospective study combined contrast-agent MRI data from various

194   patient groups to study the glymphatic function and its change with age (Zhou et al., 2020). Despite

195   different methodologies and patient cohorts from the present study, a similar age trajectory was

196   observed for the glymphatic function: it remains stable before 50 yrs and then begins to decline

197   since then (Zhou et al., 2020). The age-related glymphatic changes could be critical for the aging-

198   related risk for neurodegenerative diseases (Hou et al., 2019). The glymphatic dysfunction may

199   result in inadequate clearance and thus accumulation of toxic proteins, such as Aβ and tau, and

200   thereby increase the vulnerability to developing cognitive impairments and neurodegenerative

201   diseases (Jessen et al., 2015; Tarasoff-Conway et al., 2015). Epidemiologic research suggested the

202   late-onset AD, the most common AD variant, starts around the mid-60s with the prevalence

203   doubled every 5 years afterwards (Qiu et al., 2009). But the pathophysiological process, including

204   the accumulation of aggregated Aβ, could begin more than a decade before the dementia (Jack et

205   al., 2013; Sperling et al., 2014). Together, these findings suggested a timeline consistent with our

206   finding that the glymphatic function begins to decrease at age mid-50s.

207

208   The female sex is another leading risk factor for developing AD (Mielke et al., 2014). It has been

209   found a significantly weaker glymphatic function, as measured by gBOLD-CSF coupling strength,

210   in females than in males (Han et al., 2021b). Here we confirmed the finding with a much larger

211   dataset from healthy populations. Importantly, we further showed that the glymphatic function had

212   different age trajectories in the two groups with the females displaying a larger and more abrupt

10

213   decline at around 55 yrs. In fact, women indeed show larger and faster cognitive declines than men

214   with aging (Levine et al., 2021; Nooyens et al., 2022). Together with increasing evidence that links

215   the glymphatic dysfunction and cognitive impairments (Da Mesquita et al., 2018; Iliff et al., 2014;

216   Zou et al., 2019), the sex-specific glymphatic change with aging may provide a possible

217   explanation for the sex differences in age-related cognitive decline. The menopause and associated

218   hormone loss have been suggested to contribute to cognitive decline in females (Brown and

219   Gervais, 2020; Hachul et al., 2015). Our result is not inconsistent with this notion by showing a

220   marginally significant ($p = 0.061$) interaction between age and menopause on the coupling metrics.

221   Among the females of age 36-55, the post-menopausal group appeared to show a decline of

222   gBOLD-CSF coupling with age, which is absent in the non-menopause group. A limited sample

223   size and information related to menopause could partially account for statistical non-significance.

224   But the finding should warrant future studies looking into the menopause effects on the glymphatic

225   function with a refined design and/or augmented dataset.

226

227   Sleep quality appeared not to be a major contributor to the age-related glymphatic changes. The

228   gBOLD-CSF coupling and age are similarly correlated with a few sleep measures, including the

229   frequency of using sleep medication and the sleep troubles in the month prior to the experiments.

230   However, the age-related changes in the gBOLD-CSF coupling remained largely unchanged after

231   adjusting for these sleep measures. Nevertheless, the change in sleep architecture might be related

232   to the sex difference seen in the age-related glymphatic changes. The age and sex are known to

233   have a strong interaction effect on the composition of sleep stages. Aging in males is associated

234   with a significant increase of light sleep (stages 1&2) but decrease in slow wave sleep (SWS: sleep

235   stages 3&4), whereas this age-related change is absent in women (Mander et al., 2017; Redline et

236   al., 2004). It is known that the glymphatic function increases during sleep and anesthesia featuring

237   strong slow wave activity (SWA) (Hablitz et al., 2019; Ju et al., 2017; Xie et al., 2013), and one

238   would thus expect an improved glymphatic clearance with a higher percentage of SWS. The

239   empirical evidence, however, suggested an opposite by showing higher SWS is associated with

240   lower CSF Aβ42 level (Varga et al., 2016), which is an early indicator of preclinical AD and often

241   accompanied by cortical Aβ accumulation (Jack et al., 2013; Palmqvist et al., 2017). The paradox

242   might be explained by an observation about the gBOLD and its coupling with CSF flow. They

243   were more specifically related to ultra-slow (0.6-1 Hz) component of SWA (often related to K-

244   complexes) (Özbay et al., 2019) and phasic changes of SWA power (Fultz et al., 2019; Gu et al.,

245   2022), which could be stronger during the light sleep than SWS. Indeed, the SWA was found to

246   decrease in subjects with more cortical Aβ and poorer memory consolidation (Mander et al., 2015;

247   Winer et al., 2020), as well as AD patients (De Gennaro et al., 2017), but the reduction was specific

248   to its ultra-slow component (0.6-1 Hz) with the delta-band (1-4 Hz) power showing opposite

249   changes. Based on all these findings, it is possible that the age-related increase in the percentage

250   of light sleep in males may help to offset some age-related decline in glymphatic function and thus

251   lead to its slow deterioration as compared with females. However, the test of this hypothesis would

252   have to be left for future studies, particularly those with assessment of subjects' sleep architecture.

253

254   **STAR Methods**

255

256   **Participants and study data**

257   This study included 719 healthy human subjects (36~100 yrs; 403 females) who have participated

258   in   all   4   sessions   of   rsfMRI   scanning   in   the   HCP-A   project

12

259   (https://www.humanconnectome.org/study/hcp-lifespan-aging). For these subjects, we also used

260   their T1-weighted structural MRI imaging and demographic data, such as the age, sex, and the

261   menstrual cycle of females. These "typical aging" subjects were healthy for their age without

262   identified pathological causes of cognitive declines, such as stroke or clinical dementia

263   (Bookheimer et al., 2019). All participants provided written informed consent, and investigators

264   at each HCP-A participating site obtained ethical approval from the corresponding institutional

265   review board (IRB).

266

267   The use of de-identified data from the HCP-A and the sharing of analysis results have been

268   reviewed and approved by the Pennsylvania State University IRB (IRB#: STUDY00008766) and

269   also strictly followed the National Institute of Mental Health (NIMH) Data Archive-data use

270   certification (DUC).

271

272

273   **Image acquisition and preprocessing**

274   The rsfMRI data were acquired at 3T MR scanners (Siemens Medical Solutions; Siemens,

275   Erlangen, Germany) with a matched protocol (Harms et al., 2018) across four acquisition sites

276   including Washington University St. Louis, University of Minnesota, Massachusetts General

277   Hospital, and University of California, Los Angeles (researchers in Oxford University dedicating

278   to the data analysis). For each subject, 4 sessions of rsfMRI (including the anterior to posterior

279   phase encoding (PE) from Day1, i.e., AP1, as well as PA1, AP2, and PA2) were followed by one

280   T1-weighted structural MRI session (MPRAGE sequence, echo time (TE)= 1.8/3.6/5.4/7.2 ms

281   [multi-echo], repetition time (TR) = 2,500 ms, field of view (FOV) = 256×256 mm^2, 320×300

282   matrix, number of slices = 208, voxel size = $0.8 \times 0.8 \times 0.8$ mm^3, flip angle = 8°) (Harms et al.,

283   2018). The T1-weighted MRI served to provide the whole brain and CSF volume information and

284   was used for the anatomical segmentation and registration. For rsfMRI acquisition, 488 fMRI

285   volumes were collected with a multiband gradient-recalled (GRE) echo-planar image (EPI)

286   sequence (TR/TE=800/37 ms, flip angle=52°, FOV = 208 mm, 104×90 matrices, 72 oblique axial

287   slices, 2 mm isotropic voxels, multiband acceleration factor of 8).

288

289   We referred to the previous study (Han et al., 2021b) in preprocessing the rsfMRI data using the

290   FSL (version 5.0.9; https://fsl.fmrib.ox.ac.uk/fsl/fslwiki/FSL) (Smith et al., 2004) and AFNI

291   (version 16.3.05; https://afni.nimh.nih.gov/) (Cox, 1996). The general fMRI preprocessing

292   procedures included motion correction, skull stripping, spatial smoothing (full width at half

293   maximum (FWHM) = 4mm), temporal filtering (bandpass, approximately 0.01 to 0.1 Hz), and the

294   co-registration of each fMRI volume to corresponding T1-weighted structural MRI and then to the

295   152-brain Montreal Neurological Institute (MNI-152) space. The motion parameters were not

296   regressed out to avoid attenuating the gBOLD signal (Gu et al., 2020; Han et al., 2021b). The

297   preprocessing of structural images was performed using FSL. Processing steps included spatial

298   normalization and skull stripping.

299

Extract gBOLD and the CSF inflow signals and compute their coupling

301

302   We followed the previous studies (Han et al., 2021b, 2021a) to extract the gBOLD signal and CSF

303   inflow signal. We defined the mask of the gray matter regions based on the Harvard-Oxford

304   cortical and subcortical structural atlases (https://neurovault.org/collections/262/). We then

14

305   transformed the gray-matter mask from the MNI-152 space back to the original space of each

306   session to avoid spatial blurring from the registration process (Fultz et al., 2019), and spatially

307   averaged the Z-normalized gray-matter rsfMRI signals to obtain the gBOLD signal. Following the

308   previous study (Han et al., 2021b), the CSF inflow signal was extracted from the CSF region at

309   the bottom edge of fMRI, with a similar voxel number of CSF ROI for all subjects/sessions (see

310   an example in **Fig. S1A**). We extracted the CSF ROI from the preprocessed fMRI signal at the

311   original individual space referring to the corresponding CSF region below the bottom of the

312   cerebellum from the high-resolution T1-weighted MRI (see an exemplary time-series of gBOLD

313   and bottom CSF fMRI in **Fig. S1B**).

314

315   The cross-correlation function was calculated on the extracted gBOLD signal and the CSF inflow

316   signal for each fMRI session from each individual subject. The cross-correlation function

317   quantified the Pearson's correlation at different time lags. We first averaged all the cross-

318   correlation functions from the 4 individual fMRI sessions (AP1, PA1, AP2, and PA2) for each

319   subject, and further averaged the functions across all subjects (**Fig. S1C**). Referring to the previous

320   studies (Han et al., 2021b, 2021a), we quantified the gBOLD–CSF coupling with the session-mean

321   cross-correlation at the lag of +3.2 seconds, where the negative peak of the subject-mean cross-

322   correlation located, for each subject.

323

324   **The relationship between the gBOLD–CSF coupling and age**

325

326   To access the association between the gBOLD–CSF coupling and age, we first divided all the

327   subjects into 10 sub-groups with different ages (based on the deciles), and further calculated and

328   compared the mean gBOLD–CSF coupling for each sub-group. Moreover, all the subjects were

329   separated into the younger (age < 53.9 yrs) and older (age ≥ 53.9 yrs) groups. The linear regression

330   was used to evaluate the association between the ages and the coupling measures for the subjects

331   in each sub-group.

332

333   Several sensitivity analyses were then performed to test whether the age-coupling association

334   would be driven by the various sleep quality measures (i.e., PSQI measures), the brain volume, as

335   well as the CSF volume. We included the total PSQI score, as well as 4 different PSQI items,

336   which were selected due to their strong dependence ($p < 0.05$ for linear regression or ordinal

337   regression) with the coupling measures or age, covering the components/aspects of sleep

338   medication, trouble sleeping, and sleep hours in the sensitivity test. In the test, each of these PSQI

339   measures was first linked to the coupling measures and age, and then regressed out from the

340   coupling measures to further examine the age-coupling associations studied in **Fig. 1**. Similar age-

341   coupling association tests were applied on the whole brain volume and CSF volume, respectively.

342   The whole brain volume was accessed by the volume number of all brain regions excluding the

343   CSF area from the T1-weight MRI, where the CSF regions mainly from all the ventricles were

344   extracted to quantify the CSF volume. To test whether the head motion would drive the age-

345   coupling association, we adjusted the gBOLD-CSF coupling for the head motion from each

346   rsfMRI acquisition, which was quantified by the session-mean framewise displacement (FD),

347   following the previous study (Han et al., 2021b) and replicated the analysis in **Fig. 1**. The FD was

348   calculated as the sum of the absolute value of all 6 translational and rotational realignment

349   parameters derived from the preprocessing (Power et al., 2012). We did not use motion-censoring

16

350   methods (Power et al., 2014, 2012) to avoid the influence from the cross-correlation of the

351   concatenated timeseries of gBOLD and CSF fMRI signals.

352

353   **Sex-specific coupling changes with aging**

354

355   We further compared the gBOLD–CSF coupling strength between the male and female subjects,

356   as well as the respective trajectory of coupling changing with aging. First, we compared the

357   coupling measures between sexes with a two-sample t-test. Second, we divided the males or

358   females into 7 sub-groups (one group per 10 years; starting from 36~45 yrs, i.e., $36 \leq$ age < 46),

359   respectively, and compared the coupling measures across these sub-groups.

360

361   To examine whether the menopause would affect the tendency of the coupling measure changing

362   with aging, we separated all the females into the "post-menopause" and "other females" groups

363   (based on the measure of "whether having no period for 12 months" in the "menstrual cycle" data),

364   divided the "other females" into two stages of the "36~45 yrs" and "46~55 yrs", and compared the

365   coupling measures between the two stages. Similarly, we also selected the same age range/sub-

366   groups for the post-menopausal subjects and contrasted the corresponding coupling measures

367   between the two sub-groups, as well as compared the coupling across the "post-menopause" and

368   "other females" subjects for each age-stage. Furthermore, we applied the same grouping metric on

369   the "post-menopause" subjects as the entire group of females above, i.e., 7 groups with an age

370   duration of 10 years (from 36~45 yrs), and then replicated the analyses for whole females to

371   observe the trajectory of the coupling changing with aging.

372

17

Statistical analysis

The present study used the two-sample t-test for the group comparison of continuous variables, including the coupling difference of neighboring groups and that between males and females. The linear regression was applied to estimate the association between age and gBOLD–CSF coupling for the younger group and older group, respectively. The ordinal regression was used for responses with natural ordering among categories (i.e., the association between the coupling measure or age and these PSQI measures). The cross-correlation function was used to evaluate the relationship between the gBOLD signal and CSF inflow signal at different time lags. We also tested the interaction effects of age and menopause on the coupling measure. In the study, Pearson's correlation was employed to access the inter-subject associations between different variables. A p-value less than 0.05 was considered statistical significance.

Acknowledgements

395   Data and/or research tools used in the preparation of this manuscript were obtained from the

396   National Institute of Mental Health (NIMH) Data Archive (NDA). NDA is a collaborative

397   informatics system created by the National Institutes of Health to provide a national resource to

398   support and accelerate research in mental health. Dataset identifier(s): 10.15154/1528735. This

399   manuscript reflects the views of the authors and may not reflect the opinions or views of the NIH

400   or of the Submitters submitting original data to NDA.

401

407

408   **Author contributions:**

409

410   Conceptualization: Feng Han, Xiao Liu

411   Methodology: Feng Han, Xiao Liu

412   Investigation: Feng Han, Xufu Liu, Yifan Yang, Xiao Liu

413   Visualization: Feng Han, Yifan Yang, Xiao Liu

414   Funding acquisition: Xiao Liu

415   Project administration: Xiao Liu

416   Supervision: Xiao Liu

417   Writing – original draft: Feng Han, Xiao Liu

19

418   Writing – review & editing: Feng Han, Xufu Liu, Yifan Yang, Xiao Liu

419

420   **Competing Interests:**

421

422   The authors report no financial interests or potential conflicts of interest.

423

424   **Data and Materials Availability:**

425

426   The multimodal data, including subject characteristics, structural MRI, and rsfMRI are all publicly

427   available at the NDA website upon the approval of the data use application

428   (https://nda.nih.gov/get/access-data.html). All the code used in the present study are available from

429   the corresponding author upon request.
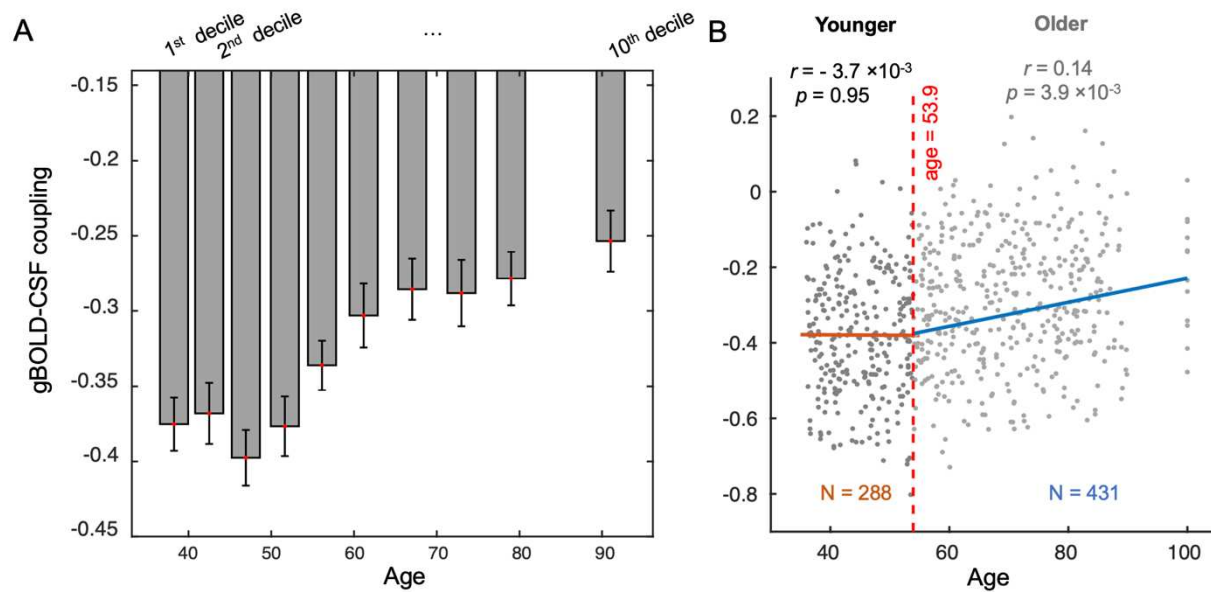
Fig. 1 The change of gBOLD–CSF coupling with age. (**A**) The gBOLD–CSF coupling remains relatively stable before age mid-50s and then begins to decrease since then. The entire cohort was grouped into 10 subgroups of equal size. Each error bar represents one standard error of the mean. (**B**) The gBOLD-CSF coupling was significantly correlated with age for the group of subjects over 53.9 yrs ($r = 0.14$, $p = 3.9 \times 10^{-3}$; gray dots at the right), but not so ($r = -3.7 \times 10^{-3}$, $p = 0.95$; black dots at the left) for the younger group. Each dot represents one subject.
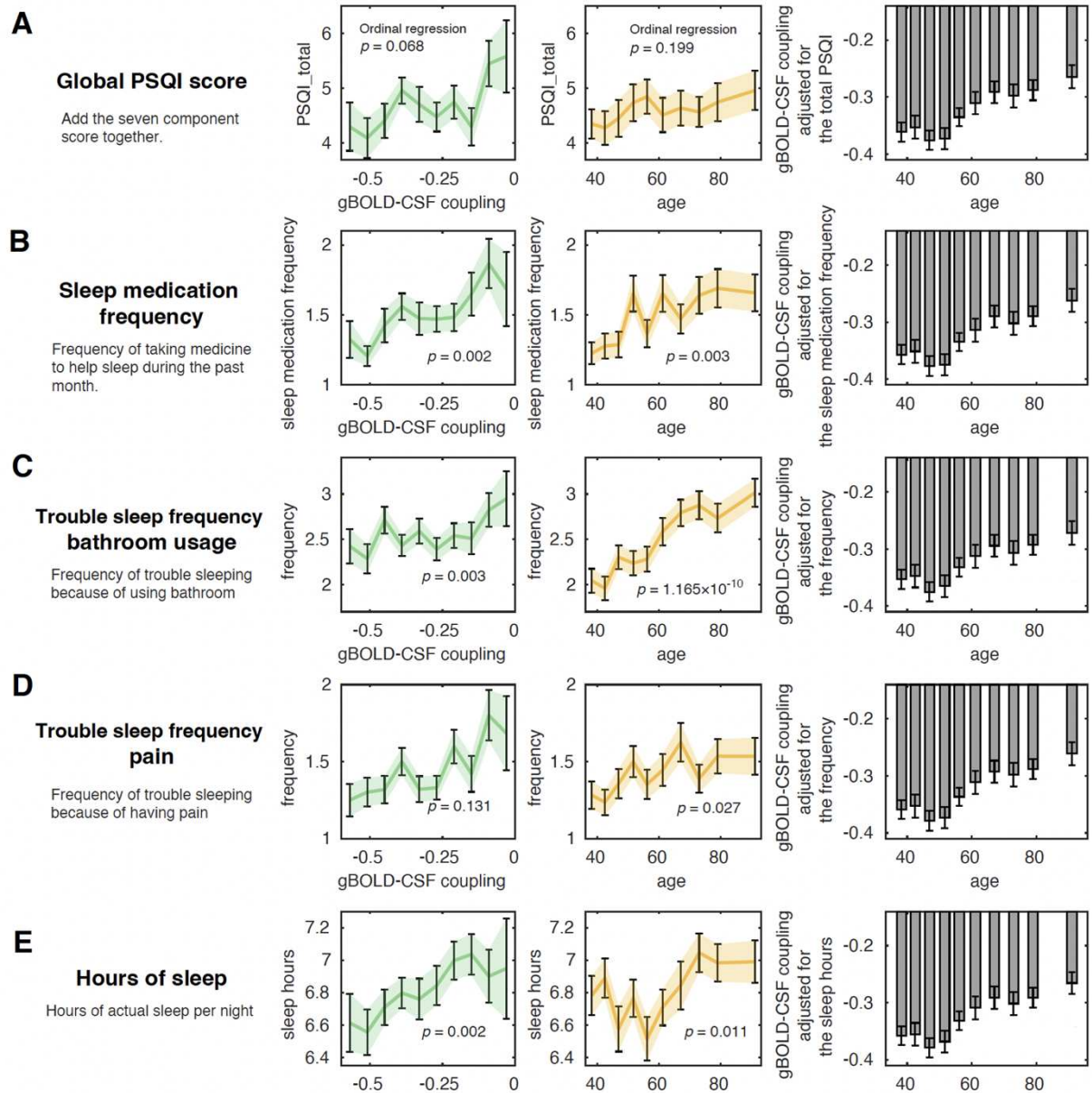
21

437

Fig. 2 The age-related changes in gBOLD-CSF coupling remain similar with controlling for sleep measures. The gBOLD-CSF coupling (left) and age (middle) are similarly correlated with a few sleep-related measurements in PSQI, including the sleep medication frequency (2nd row), the frequency of bathroom-use during sleep-time (3rd row), the frequency of having pain during sleep-time (4th row), and sleep hours (5th row), but not the total PSQI score (1st row). However, the

444   age-related changes in gBOLD-CSF coupling remain similar with adjusting for these PSQI

445   measures (right). Each dot represents one subject, and error bars represent the standard error of the
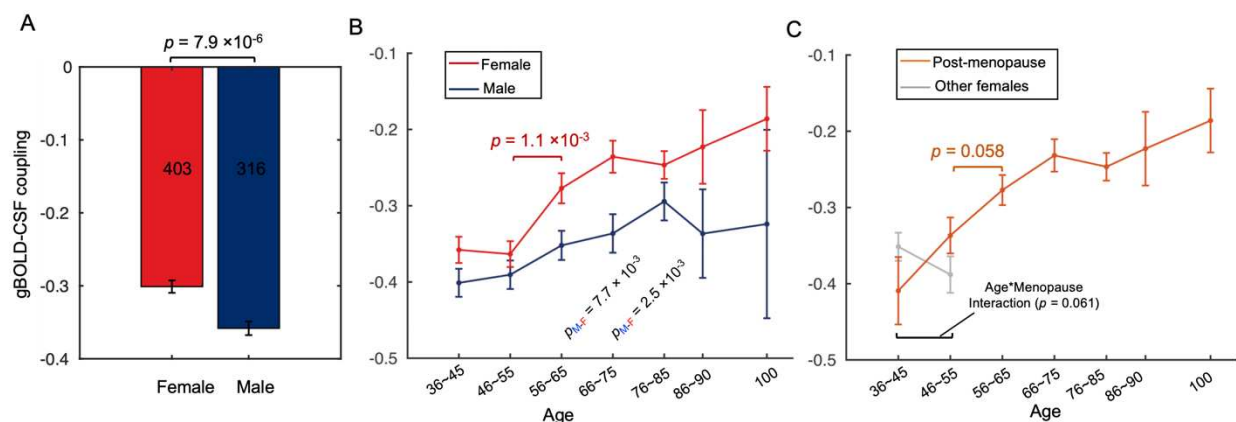
446   mean.

447

448

449

450 **Fig. 3 The age-coupling association showed distinct patterns between males and females. (A)**

451 The gBOLD-CSF coupling is significantly weaker in females (red) than in males (blue) ($p = $

452 7.9×10^{-6}, two-sample t-test). (**B**) The age-related changes of the gBOLD-CSF coupling were

453 summarized separately for the females and males and showed different patterns of trajectory:

454 gBOLD–CSF coupling in the females showed a steep decline around 55 yrs ($p = 1.1 \times 10^{-3}$ for two

455 consecutive subgroups around that age), in contrast to the slow and gradual decreases in the males.

456 (**C**) The gBOLD-CSF coupling trends in the "Post-menopause" and "Other females" groups. All

457 females above age 55 are post-menopause. Within the age range of 36-55, the menopause status

458 and age showed a marginally significant ($p = 0.061$) interaction effect on the gBOLD-CSF

459 coupling. The coupling index started to decrease early at age mid-40s and thus its reduction around

460 age mid-50s is less significant ($p = 0.058$) as compared with the entire female group.

461

24

462   **References**

463   Abbott, N.J., Pizzo, M.E., Preston, J.E., Janigro, D., Thorne, R.G., 2018. The role of brain

464   barriers in fluid movement in the CNS: is there a 'glymphatic' system? Acta Neuropathol.

465   135, 387–407. https://doi.org/10.1007/s00401-018-1812-4

466   Baust, W., Bohnert, B., 1969. The regulation of heart rate during sleep. Exp. Brain Res.

467   https://doi.org/10.1007/BF00235442

468   Benveniste, H., Liu, X., Koundal, S., Sanggaard, S., Lee, H., Wardlaw, J., 2019. The Glymphatic

469   System and Waste Clearance with Brain Aging: A Review. Gerontology 65, 106–119.

470   https://doi.org/10.1159/000490349

471   Birn, R.M., Diamond, J.B., Smith, M.A., Bandettini, P.A., 2006. Separating respiratory-

472   variation-related fluctuations from neuronal-activity-related fluctuations in fMRI.

473   Neuroimage. https://doi.org/10.1016/j.neuroimage.2006.02.048

474   Boland, B., Yu, W.H., Corti, O., Mollereau, B., Henriques, A., Bezard, E., Pastores, G.M.,

475   Rubinsztein, D.C., Nixon, R.A., Duchen, M.R., Mallucci, G.R., Kroemer, G., Levine, B.,

476   Eskelinen, E.-L., Mochel, F., Spedding, M., Louis, C., Martin, O.R., Millan, M.J., 2018.

477   Promoting the clearance of neurotoxic proteins in neurodegenerative disorders of ageing.

478   Nat. Rev. Drug Discov. 17, 660–688. https://doi.org/10.1038/nrd.2018.109

479   Bookheimer, S.Y., Salat, D.H., Terpstra, M., Ances, B.M., Barch, D.M., Buckner, R.L., Burgess,

480   G.C., Curtiss, S.W., Diaz-Santos, M., Elam, J.S., Fischl, B., Greve, D.N., Hagy, H.A.,

481   Harms, M.P., Hatch, O.M., Hedden, T., Hodge, C., Japardi, K.C., Kuhn, T.P., Ly, T.K.,

482   Smith, S.M., Somerville, L.H., Uğurbil, K., van der Kouwe, A., Van Essen, D., Woods,

483   R.P., Yacoub, E., 2019. The Lifespan Human Connectome Project in Aging: An overview.

484   Neuroimage 185, 335–348. https://doi.org/10.1016/j.neuroimage.2018.10.009

485   Boudreau, P., Yeh, W.H., Dumont, G.A., Boivin, D.B., 2013. Circadian variation of heart rate

486   variability across sleep stages. Sleep. https://doi.org/10.5665/sleep.3230

487   Brown, A.M.C., Gervais, N.J., 2020. Role of Ovarian Hormones in the Modulation of Sleep in

488   Females Across the Adult Lifespan. Endocrinology 161.

489   https://doi.org/10.1210/endocr/bqaa128

490   Chang, C., Cunningham, J.P., Glover, G.H., 2009. Influence of heart rate on the BOLD signal:

491   The cardiac response function. Neuroimage.

492   https://doi.org/10.1016/j.neuroimage.2008.09.029

493   Chen, R.L., Kassem, N.A., Redzic, Z.B., Chen, C.P.C., Segal, M.B., Preston, J.E., 2009. Age-

494   related changes in choroid plexus and blood–cerebrospinal fluid barrier function in the

495   sheep. Exp. Gerontol. 44, 289–296.

496   https://doi.org/https://doi.org/10.1016/j.exger.2008.12.004

497   Cox, R.W., 1996. AFNI: Software for analysis and visualization of functional magnetic

498   resonance neuroimages. Comput. Biomed. Res. https://doi.org/10.1006/cbmr.1996.0014

499   Da Mesquita, S., Louveau, A., Vaccari, A., Smirnov, I., Cornelison, R.C., Kingsmore, K.M.,

500   Contarino, C., Onengut-Gumuscu, S., Farber, E., Raper, D., Viar, K.E., Powell, R.D.,

501   Baker, W., Dabhi, N., Bai, R., Cao, R., Hu, S., Rich, S.S., Munson, J.M., Lopes, M.B.,

502   Overall, C.C., Acton, S.T., Kipnis, J., 2018. Functional aspects of meningeal lymphatics in

503   ageing and Alzheimer's disease. Nature 560, 185–191. https://doi.org/10.1038/s41586-018-

504   0368-8

505   De Gennaro, L., Gorgoni, M., Reda, F., Lauri, G., Truglia, I., Cordone, S., Scarpelli, S.,

506   Mangiaruga, A., D'atri, A., Lacidogna, G., Ferrara, M., Marra, C., Rossini, P.M., 2017. The

507   Fall of Sleep K-Complex in Alzheimer Disease. Sci. Rep. 7, 39688.

508   https://doi.org/10.1038/srep39688

509   Douglas, N.J., White, D.P., Pickett, C.K., Weil, J. V., Zwillich, C.W., 1982. Respiration during

510   sleep in normal man. Thorax. https://doi.org/10.1136/thx.37.11.840

511   Eide, P.K., Vatnehol, S.A.S., Emblem, K.E., Ringstad, G., 2018. Magnetic resonance imaging

512   provides evidence of glymphatic drainage from human brain to cervical lymph nodes. Sci.

513   Rep. 8, 7194. https://doi.org/10.1038/s41598-018-25666-4

514   Fleischman, D., Berdahl, J.P., Zaydlarova, J., Stinnett, S., Fautsch, M.P., Allingham, R.R., 2012.

515   Cerebrospinal Fluid Pressure Decreases with Older Age. PLoS One 7, 1–9.

516   https://doi.org/10.1371/journal.pone.0052664

517   Fukunaga, M., Horovitz, S.G., van Gelderen, P., de Zwart, J.A., Jansma, J.M., Ikonomidou,

518   V.N., Chu, R., Deckers, R.H.R., Leopold, D.A., Duyn, J.H., 2006. Large-amplitude,

519   spatially correlated fluctuations in BOLD fMRI signals during extended rest and early sleep

520   stages. Magn. Reson. Imaging 24, 979–992. https://doi.org/10.1016/j.mri.2006.04.018

521   Fultz, N.E., Bonmassar, G., Setsompop, K., Stickgold, R.A., Rosen, B.R., Polimeni, J.R., Lewis,

522   L.D., 2019. Coupled electrophysiological, hemodynamic, and cerebrospinal fluid

523   oscillations in human sleep. Science (80-.). https://doi.org/10.1126/science.aax5440

524   Gao, J.H., Liu, H.L., 2012. Inflow effects on functional MRI. Neuroimage.

525   https://doi.org/10.1016/j.neuroimage.2011.09.088

526   Gao, J.H., Miller, I., Lai, S., Xiong, J., Fox, P.T., 1996. Quantitative assessment of blood inflow

527   effects in functional MRI signals. Magn. Reson. Med.

528   https://doi.org/10.1002/mrm.1910360219

529   Gu, Y., Han, F., Sainburg, L.E., Liu, X., 2020. Transient Arousal Modulations Contribute to

530   Resting-State Functional Connectivity Changes Associated with Head Motion Parameters.

531   Cereb. Cortex. https://doi.org/10.1093/cercor/bhaa096

532 Gu, Y., Han, F., Sainburg, L.E., Schade, M.M., Buxton, O.M., Duyn, J.H., Liu, X., 2022. An

533   orderly sequence of autonomic and neural events at transient arousal changes. Neuroimage.

534   https://doi.org/10.1016/j.neuroimage.2022.119720

535 Gu, Y., Sainburg, L.E., Kuang, S., Han, F., Williams, J.W., Liu, Y., Zhang, N., Zhang, X.,

536   Leopold, D.A., Liu, X., 2021. Brain Activity Fluctuations Propagate as Waves Traversing

537   the Cortical Hierarchy. Cereb. Cortex 31, 3986–4005.

538   https://doi.org/10.1093/cercor/bhab064

539 Guazzi, M., Zanchetti, A., 1965. Carotid sinus and aortic reflexes in the regulation of circulation

540   during sleep. Science (80-.). https://doi.org/10.1126/science.148.3668.397

541 Hablitz, L.M., Vinitsky, H.S., Sun, Q., Stæger, F.F., Sigurdsson, B., Mortensen, K.N., Lilius,

542   T.O., Nedergaard, M., 2019. Increased glymphatic influx is correlated with high EEG delta

543   power and low heart rate in mice under anesthesia. Sci. Adv. 5, eaav5447.

544   https://doi.org/10.1126/sciadv.aav5447

545 Hachul, H., Frange, C., Bezerra, A.G., Hirotsu, C., Pires, G.N., Andersen, M.L., Bittencourt, L.,

546   Tufik, S., 2015. The effect of menopause on objective sleep parameters: Data from an

547   epidemiologic study in São Paulo, Brazil. Maturitas 80, 170–178.

548   https://doi.org/https://doi.org/10.1016/j.maturitas.2014.11.002

549 Han, F., Brown, G.L., Zhu, Y., Belkin-Rosen, A.E., Lewis, M.M., Du, G., Gu, Y., Eslinger, P.J.,

550   Mailman, R.B., Huang, X., Liu, X., 2021a. Decoupling of Global Brain Activity and

551   Cerebrospinal Fluid Flow in Parkinson's Disease Cognitive Decline. Mov. Disord. 36,

552   2066–2076. https://doi.org/10.1002/mds.28643

553 Han, F., Chen, J., Belkin-Rosen, A., Gu, Y., Luo, L., Buxton, O.M., Liu, X., 2021b. Reduced

554   coupling between cerebrospinal fluid flow and global brain activity is linked to Alzheimer

555   disease–related pathology. PLoS Biol. 19, 1–25.

556   https://doi.org/10.1371/journal.pbio.3001233

557 Han, F., Liu, Xufu, Mailman, R.B., Huang, X., Liu, Xiao, 2022. Early β-amyloid accumulation

558   and hypoconnectivity in the default mode network are related to its disengagement from

559   global brain activity. bioRxiv. https://doi.org/10.1101/2022.07.24.501309

560 Harms, M.P., Somerville, L.H., Ances, B.M., Andersson, J., Barch, D.M., Bastiani, M.,

561   Bookheimer, S.Y., Brown, T.B., Buckner, R.L., Burgess, G.C., Coalson, T.S., Chappell,

562   M.A., Dapretto, M., Douaud, G., Fischl, B., Glasser, M.F., Greve, D.N., Hodge, C.,

563   Jamison, K.W., Jbabdi, S., Kandala, S., Li, X., Mair, R.W., Mangia, S., Marcus, D.,

564   Mascali, D., Moeller, S., Nichols, T.E., Robinson, E.C., Salat, D.H., Smith, S.M.,

565   Sotiropoulos, S.N., Terpstra, M., Thomas, K.M., Tisdall, M.D., Ugurbil, K., van der

566   Kouwe, A., Woods, R.P., Zöllei, L., Van Essen, D.C., Yacoub, E., 2018. Extending the

567   Human Connectome Project across ages: Imaging protocols for the Lifespan Development

568   and Aging projects. Neuroimage 183, 972–984.

569   https://doi.org/10.1016/j.neuroimage.2018.09.060

570 Helakari, H., Korhonen, V., Holst, S.C., Piispala, J., Kallio, M., Väyrynen, T., Huotari, N.,

571   Raitamaa, L., Tuunanen, J., Kananen, J., Järvelä, M., Tuovinen, T., Raatikainen, V.,

572   Borchardt, V., Kinnunen, H., Nedergaard, M., Kiviniemi, V., 2022. Human NREM Sleep

573   Promotes Brain-Wide Vasomotor and Respiratory Pulsations. J. Neurosci. JN-RM-0934-21.

574   https://doi.org/10.1523/jneurosci.0934-21.2022

575 Hladky, S.B., Barrand, M.A., 2022. The glymphatic hypothesis: the theory and the evidence,

576   Fluids and Barriers of the CNS. BioMed Central. https://doi.org/10.1186/s12987-021-

577   00282-z

578   Holth, J.K., Fritschi, S.K., Wang, C., Pedersen, N.P., Cirrito, J.R., Mahan, T.E., Finn, M.B.,

579   Manis, M., Geerling, J.C., Fuller, P.M., Lucey, B.P., Holtzman, D.M., 2019. The sleep-

580   wake cycle regulates brain interstitial fluid tau in mice and CSF tau in humans. Science

581   (80-.). https://doi.org/10.1126/science.aav2546

582   Hou, Y., Dan, X., Babbar, M., Wei, Y., Hasselbalch, S.G., Croteau, D.L., Bohr, V.A., 2019.

583   Ageing as a risk factor for neurodegenerative disease. Nat. Rev. Neurol. 15, 565–581.

584   https://doi.org/10.1038/s41582-019-0244-7

585   Iliff, J.J., Chen, M.J., Plog, B.A., Zeppenfeld, D.M., Soltero, M., Yang, L., Singh, I., Deane, R.,

586   Nedergaard, M., 2014. Impairment of glymphatic pathway function promotes tau pathology

587   after traumatic brain injury. J. Neurosci. https://doi.org/10.1523/JNEUROSCI.3020-14.2014

588   Iliff, J.J., Wang, M., Liao, Y., Plogg, B.A., Peng, W., Gundersen, G.A., Benveniste, H., Vates,

589   G.E., Deane, R., Goldman, S.A., Nagelhus, E.A., Nedergaard, M., 2012. A paravascular

590   pathway facilitates CSF flow through the brain parenchyma and the clearance of interstitial

591   solutes, including amyloid β. Sci. Transl. Med.

592   https://doi.org/10.1126/scitranslmed.3003748

593   Iliff, J.J., Wang, M., Zeppenfeld, D.M., Venkataraman, A., Plog, B.A., Liao, Y., Deane, R.,

594   Nedergaard, M., 2013. Cerebral arterial pulsation drives paravascular CSF-Interstitial fluid

595   exchange in the murine brain. J. Neurosci. https://doi.org/10.1523/JNEUROSCI.1592-

596   13.2013

597   Jack, C.R., Knopman, D.S., Jagust, W.J., Petersen, R.C., Weiner, M.W., Aisen, P.S., Shaw,

598   L.M., Vemuri, P., Wiste, H.J., Weigand, S.D., Lesnick, T.G., Pankratz, V.S., Donohue,

599   M.C., Trojanowski, J.Q., 2013. Tracking pathophysiological processes in Alzheimer's

600   disease: An updated hypothetical model of dynamic biomarkers. Lancet Neurol. 12, 207–

601   216. https://doi.org/10.1016/S1474-4422(12)70291-0

602 Jessen, N.A., Munk, A.S.F., Lundgaard, I., Nedergaard, M., 2015. The Glymphatic System: A

603   Beginner's Guide. Neurochem. Res. https://doi.org/10.1007/s11064-015-1581-6

604 Ju, Y.-E.S., Ooms, S.J., Sutphen, C., Macauley, S.L., Zangrilli, M.A., Jerome, G., Fagan, A.M.,

605   Mignot, E., Zempel, J.M., Claassen, J.A.H.R., Holtzman, D.M., 2017. Slow wave sleep

606   disruption increases cerebrospinal fluid amyloid-β levels. Brain 140, 2104–2111.

607   https://doi.org/10.1093/brain/awx148

608 Kiviniemi, V., Wang, X., Korhonen, V., Keinänen, T., Tuovinen, T., Autio, J., Levan, P.,

609   Keilholz, S., Zang, Y.F., Hennig, J., Nedergaard, M., 2016. Ultra-fast magnetic resonance

610   encephalography of physiological brain activity-Glymphatic pulsation mechanisms? J.

611   Cereb. Blood Flow Metab. https://doi.org/10.1177/0271678X15622047

612 Kress, B.T., Iliff, J.J., Xia, M., Wang, M., Wei Bs, H.S., Zeppenfeld, D., Xie, L., Hongyi Kang,

613   B.S., Xu, Q., Liew, J.A., Plog, B.A., Ding, F., PhD, R.D., Nedergaard, M., 2014.

614   Impairment of paravascular clearance pathways in the aging brain. Ann. Neurol. 76, 845–

615   861. https://doi.org/10.1002/ana.24271

616 Larson-Prior, L.J., Zempel, J.M., Nolan, T.S., Prior, F.W., Snyder, A., Raichle, M.E., 2009.

617   Cortical network functional connectivity in the descent to sleep. Proc. Natl. Acad. Sci. U. S.

618   A. https://doi.org/10.1073/pnas.0900924106

619 Levine, D.A., Gross, A.L., Briceño, E.M., Tilton, N., Giordani, B.J., Sussman, J.B., Hayward,

620   R.A., Burke, J.F., Hingtgen, S., Elkind, M.S.V., Manly, J.J., Gottesman, R.F., Gaskin, D.J.,

621   Sidney, S., Sacco, R.L., Tom, S.E., Wright, C.B., Yaffe, K., Galecki, A.T., 2021. Sex

622   Differences in Cognitive Decline among US Adults. JAMA Netw. Open 4, 1–13.

623   https://doi.org/10.1001/jamanetworkopen.2021.0169

624   Liu, X., De Zwart, J.A., Schölvinck, M.L., Chang, C., Ye, F.Q., Leopold, D.A., Duyn, J.H.,

625   2018. Subcortical evidence for a contribution of arousal to fMRI studies of brain activity.

626   Nat. Commun. https://doi.org/10.1038/s41467-017-02815-3

627   Liu, X., Leopold, D.A., Yang, Y., 2021. Single-neuron firing cascades underlie global

628   spontaneous brain events. Proc. Natl. Acad. Sci. U. S. A. 118, 1–10.

629   https://doi.org/10.1073/pnas.2105395118

630   Liu, X., Yanagawa, T., Leopold, D.A., Chang, C., Ishida, H., Fujii, N., Duyn, J.H., 2015.

631   Arousal transitions in sleep, wakefulness, and anesthesia are characterized by an orderly

632   sequence of cortical events. Neuroimage. https://doi.org/10.1016/j.neuroimage.2015.04.003

633   Mander, B.A., Marks, S.M., Vogel, J.W., Rao, V., Lu, B., Saletin, J.M., Ancoli-Israel, S., Jagust,

634   W.J., Walker, M.P., 2015. β-amyloid disrupts human NREM slow waves and related

635   hippocampus-dependent memory consolidation. Nat. Neurosci. 18, 1051–1057.

636   https://doi.org/10.1038/nn.4035

637   Mander, B.A., Winer, J.R., Walker, M.P., 2017. Sleep and Human Aging. Neuron 94, 19–36.

638   https://doi.org/https://doi.org/10.1016/j.neuron.2017.02.004

639   Mawuenyega, K.G., Sigurdson, W., Ovod, V., Munsell, L., Kasten, T., Morris, J.C., Yarasheski,

640   K.E., Bateman, R.J., 2010. Decreased clearance of CNS β-amyloid in Alzheimer's disease.

641   Science (80-.). 330, 1774. https://doi.org/10.1126/science.1197623

642   Mestre, H., Tithof, J., Du, T., Song, W., Peng, W., Sweeney, A.M., Olveda, G., Thomas, J.H.,

643   Nedergaard, M., Kelley, D.H., 2018. Flow of cerebrospinal fluid is driven by arterial

644   pulsations and is reduced in hypertension. Nat. Commun. https://doi.org/10.1038/s41467-

645   018-07318-3

646 Mielke, M.M., Vemuri, P., Rocca, W.A., 2014. Clinical epidemiology of Alzheimer's disease:

647   Assessing sex and gender differences. Clin. Epidemiol.

648   https://doi.org/10.2147/CLEP.S37929

649 Nedergaard, M., Goldman, S.A., 2020. Glymphatic failure as a final common pathway to

650   dementia. Science (80-.). 370, 50–56. https://doi.org/10.1126/science.abb8739

651 Nooyens, A.C.J., Wijnhoven, H.A.H., Schaap, L.S., Sialino, L.D., Kok, A.A.L., Visser, M.,

652   Verschuren, W.M.M., Picavet, H.S.J., van Oostrom, S.H., 2022. Sex Differences in

653   Cognitive Functioning with Aging in the Netherlands. Gerontology.

654   https://doi.org/10.1159/000520318

655 Olbrich, S., Mulert, C., Karch, S., Trenner, M., Leicht, G., Pogarell, O., Hegerl, U., 2009. EEG-

656   vigilance and BOLD effect during simultaneous EEG/fMRI measurement. Neuroimage.

657   https://doi.org/10.1016/j.neuroimage.2008.11.014

658 Özbay, P.S., Chang, C., Picchioni, D., Mandelkow, H., Chappel-Farley, M.G., van Gelderen, P.,

659   de Zwart, J.A., Duyn, J., 2019. Sympathetic activity contributes to the fMRI signal.

660   Commun. Biol. https://doi.org/10.1038/s42003-019-0659-0

661 Özbay, P.S., Chang, C., Picchioni, D., Mandelkow, H., Moehlman, T.M., Chappel-Farley, M.G.,

662   van Gelderen, P., de Zwart, J.A., Duyn, J.H., 2018. Contribution of systemic vascular

663   effects to fMRI activity in white matter. Neuroimage.

664   https://doi.org/10.1016/j.neuroimage.2018.04.045

665 Pais-Roldán, P., Takahashi, K., Sobczak, F., Chen, Y., Zhao, X., Zeng, H., Jiang, Y., Yu, X.,

666   2020. Indexing brain state-dependent pupil dynamics with simultaneous fMRI and optical

667   fiber calcium recording. Proc. Natl. Acad. Sci. U. S. A. 117, 6875–6882.

668   https://doi.org/10.1073/pnas.1909937117

669   Palmqvist, S., Schöll, M., Strandberg, O., Mattsson, N., Stomrud, E., Zetterberg, H., Blennow,

670   K., Landau, S., Jagust, W., Hansson, O., 2017. Earliest accumulation of β-amyloid occurs

671   within the default-mode network and concurrently affects brain connectivity. Nat. Commun.

672   https://doi.org/10.1038/s41467-017-01150-x

673   Peng, W., Achariyar, T.M., Li, B., Liao, Y., Mestre, H., Hitomi, E., Regan, S., Kasper, T., Peng,

674   S., Ding, F., Benveniste, H., Nedergaard, M., Deane, R., 2016. Suppression of glymphatic

675   fluid transport in a mouse model of Alzheimer's disease. Neurobiol. Dis. 93, 215–225.

676   https://doi.org/https://doi.org/10.1016/j.nbd.2016.05.015

677   Power, J.D., Barnes, K.A., Snyder, A.Z., Schlaggar, B.L., Petersen, S.E., 2012. Spurious but

678   systematic correlations in functional connectivity MRI networks arise from subject motion.

679   Neuroimage. https://doi.org/10.1016/j.neuroimage.2011.10.018

680   Power, J.D., Mitra, A., Laumann, T.O., Snyder, A.Z., Schlaggar, B.L., Petersen, S.E., 2014.

681   Methods to detect, characterize, and remove motion artifact in resting state fMRI.

682   Neuroimage 84, 320–341. https://doi.org/10.1016/j.neuroimage.2013.08.048

683   Power, J.D., Plitt, M., Gotts, S.J., Kundu, P., Voon, V., Bandettini, P.A., Martin, A., 2018.

684   Ridding fMRI data of motion-related influences: Removal of signals with distinct spatial

685   and physical bases in multiecho data. Proc. Natl. Acad. Sci. U. S. A.

686   https://doi.org/10.1073/pnas.1720985115

687   Qiu, C., Kivipelto, M., von Strauss, E., 2009. Epidemiology of Alzheimer's disease: occurrence,

688   determinants, and strategies toward intervention. Dialogues Clin. Neurosci. 11, 111–128.

689   https://doi.org/10.31887/DCNS.2009.11.2/cqiu

690   Raut, R. V., Snyder, A.Z., Mitra, A., Yellin, D., Fujii, N., Malach, R., Raichle, M.E., 2021.

691   Global waves synchronize the brain's functional systems with fluctuating arousal. Sci. Adv.

692   7, 1–16. https://doi.org/10.1126/sciadv.abf2709

693   Redline, S., Kirchner, H.L., Quan, S.F., Gottlieb, D.J., Kapur, V., Newman, A., 2004. The

694   Effects of Age, Sex, Ethnicity, and Sleep-Disordered Breathing on Sleep Architecture.

695   Arch. Intern. Med. 164, 406–418. https://doi.org/10.1001/archinte.164.4.406

696   Smith, S.M., Jenkinson, M., Woolrich, M.W., Beckmann, C.F., Behrens, T.E.J., Johansen-Berg,

697   H., Bannister, P.R., De Luca, M., Drobnjak, I., Flitney, D.E., Niazy, R.K., Saunders, J.,

698   Vickers, J., Zhang, Y., De Stefano, N., Brady, J.M., Matthews, P.M., 2004. Advances in

699   functional and structural MR image analysis and implementation as FSL. Neuroimage 23,

700   S208–S219. https://doi.org/https://doi.org/10.1016/j.neuroimage.2004.07.051

701   Snyder, F., Hobson, J.A., Morrison, D.F., Goldfrank, F., 1964. Changes in respiration, heart rate,

702   and systolic blood pressure in human sleep. J. Appl. Physiol.

703   https://doi.org/10.1152/jappl.1964.19.3.417

704   Sperling, R., Mormino, E., Johnson, K., 2014. The evolution of preclinical Alzheimer's disease:

705   Implications for prevention trials. Neuron. https://doi.org/10.1016/j.neuron.2014.10.038

706   Tarasoff-Conway, J.M., Carare, R.O., Osorio, R.S., Glodzik, L., Butler, T., Fieremans, E., Axel,

707   L., Rusinek, H., Nicholson, C., Zlokovic, B. V., Frangione, B., Blennow, K., Ménard, J.,

708   Zetterberg, H., Wisniewski, T., De Leon, M.J., 2015. Clearance systems in the brain -

709   Implications for Alzheimer disease. Nat. Rev. Neurol.

710   https://doi.org/10.1038/nrneurol.2015.119

711   Thompson, G.J., Pan, W.-J., Magnuson, M.E., Jaeger, D., Keilholz, S.D., 2014. Quasi-periodic

712   patterns (QPP): Large-scale dynamics in resting state fMRI that correlate with local

713   infraslow electrical activity. Neuroimage 84, 1018–1031.

714   https://doi.org/https://doi.org/10.1016/j.neuroimage.2013.09.029

715   Turchi, J., Chang, C., Ye, F.Q., Russ, B.E., Yu, D.K., Cortes, C.R., Monosov, I.E., Duyn, J.H.,

716   Leopold, D.A., 2018. The Basal Forebrain Regulates Global Resting-State fMRI

717   Fluctuations. Neuron. https://doi.org/10.1016/j.neuron.2018.01.032

718   Turner, K.L., Gheres, K.W., Drew, P.J., 2022. Relating Pupil Diameter and Blinking to Cortical

719   Activity and Hemodynamics across Arousal States. Journal of Neuroscience.

720   https://doi.org/10.1523/JNEUROSCI.1244-22.2022

721   Turner, K.L., Gheres, K.W., Proctor, E.A., Drew, P.J., 2020. Neurovascular coupling and

722   bilateral connectivity during NREM and REM sleep. Elife 9, e62071.

723   https://doi.org/10.7554/eLife.62071

724   van Veluw, S.J., Hou, S.S., Calvo-Rodriguez, M., Arbel-Ornath, M., Snyder, A.C., Frosch, M.P.,

725   Greenberg, S.M., Bacskai, B.J., 2020. Vasomotion as a Driving Force for Paravascular

726   Clearance in the Awake Mouse Brain. Neuron.

727   https://doi.org/10.1016/j.neuron.2019.10.033

728   Varga, A.W., Wohlleber, M.E., Giménez, S., Romero, S., Alonso, J.F., Ducca, E.L., Kam, K.,

729   Lewis, C., Tanzi, E.B., Tweardy, S., Kishi, A., Parekh, A., Fischer, E., Gumb, T., Alcolea,

730   D., Fortea, J., Lleó, A., Blennow, K., Zetterberg, H., Mosconi, L., Glodzik, L., Pirraglia, E.,

731   Burschtin, O.E., de Leon, M.J., Rapoport, D.M., Lu, S., Ayappa, I., Osorio, R.S., 2016.

732   Reduced Slow-Wave Sleep Is Associated with High Cerebrospinal Fluid Aβ42 Levels in

733   Cognitively Normal Elderly. Sleep 39, 2041–2048. https://doi.org/10.5665/sleep.6240

734   Wang, M., He, Y., Sejnowski, T.J., Yu, X., 2018. Brain-state dependent astrocytic Ca2+ signals

735   are coupled to both positive and negative BOLD-fMRI signals. Proc. Natl. Acad. Sci. U. S.

736   A. 115, E1647–E1656. https://doi.org/10.1073/pnas.1711692115

737   Winer, J.R., Mander, B.A., Kumar, S., Reed, M., Baker, S.L., Jagust, W.J., Walker, M.P., 2020.

738   Sleep Disturbance Forecasts β-Amyloid Accumulation across Subsequent Years. Curr. Biol.

739   30, 4291-4298.e3. https://doi.org/10.1016/j.cub.2020.08.017

740   Xie, L., Kang, H., Xu, Q., Chen, M.J., Liao, Y., Thiyagarajan, M., O'Donnell, J., Christensen,

741   D.J., Nicholson, C., Iliff, J.J., Takano, T., Deane, R., Nedergaard, M., 2013. Sleep drives

742   metabolite clearance from the adult brain. Science (80-.).

743   https://doi.org/10.1126/science.1241224

744   Yamada, S., Miyazaki, M., Yamashita, Y., Ouyang, C., Yui, M., Nakahashi, M., Shimizu, S.,

745   Aoki, I., Morohoshi, Y., McComb, J.G., 2013. Influence of respiration on cerebrospinal

746   fluid movement using magnetic resonance spin labeling. Fluids Barriers CNS.

747   https://doi.org/10.1186/2045-8118-10-36

748   Zhou, Y., Cai, J., Zhang, W., Gong, X., Yan, S., Zhang, K., Luo, Z., Sun, J., Jiang, Q., Lou, M.,

749   2020. Impairment of the Glymphatic Pathway and Putative Meningeal Lymphatic Vessels

750   in the Aging Human. Ann. Neurol. 87, 357–369.

751   https://doi.org/https://doi.org/10.1002/ana.25670

752   Zieman, S.J., Melenovsky, V., Kass, D.A., 2005. Mechanisms, Pathophysiology, and Therapy of

753   Arterial Stiffness. Arterioscler. Thromb. Vasc. Biol. 25, 932–943.

754   https://doi.org/10.1161/01.ATV.0000160548.78317.29

755   Zou, W., Pu, T., Feng, W., Lu, M., Zheng, Y., Du, R., Xiao, M., Hu, G., 2019. Blocking

756   meningeal lymphatic drainage aggravates Parkinson's disease-like pathology in mice

757   overexpressing mutated α-synuclein. Transl. Neurodegener. 8, 7.

758   https://doi.org/10.1186/s40035-019-0147-y

759

760

761

762

763

Supplementary Materials

765   **Fig. S1** to **S4** for multiple supplementary figures
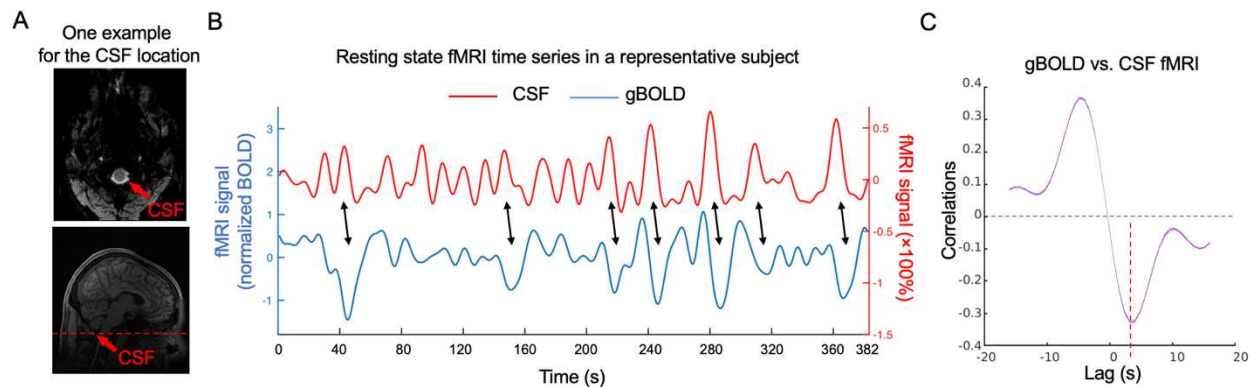
766

767

768

Fig. S1 gBOLD is coupled with CSF changes in HCP-Aging data. (**A**) **Top**: CSF region at bottom fMRI slice shown in an example subject; **Bottom**: location of bottom rsfMRI slice marked in corresponding structural MRI (dashed line). (**B**) gBOLD (blue) and CSF (red) rsfMRI signals showed a coupled change (black arrows) from a representative example. (**C**) Averaged cross-correlation function between gBOLD and CSF across 719 subjects. The red dashed line marks the time lag (+3.2-sec) where the negative peak of the mean cross-correlation occurs. The shaded regions represent the area within one standard error of the mean.
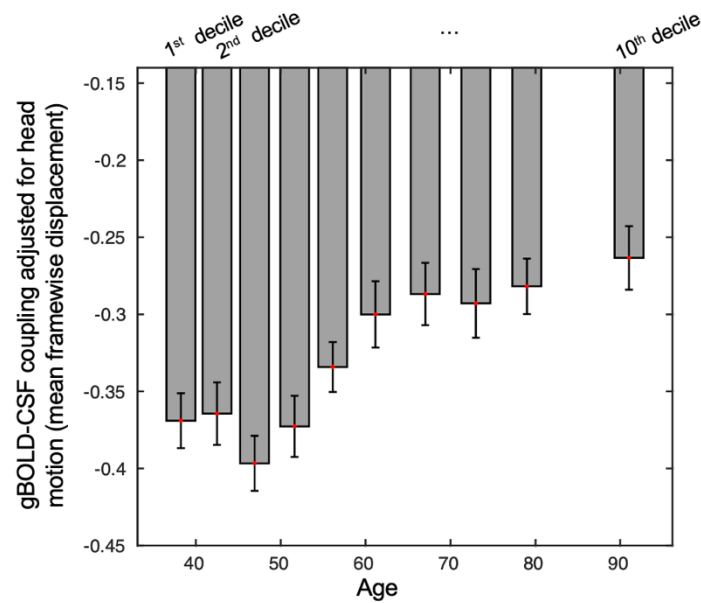
776

777

778

Fig. S2 The age-coupling association was not affected by head motion during fMRI acquisition. Similar results as **Fig.1** were found when the mean FD was regressed out from the gBOLD-CSF coupling for each rsfMRI session.
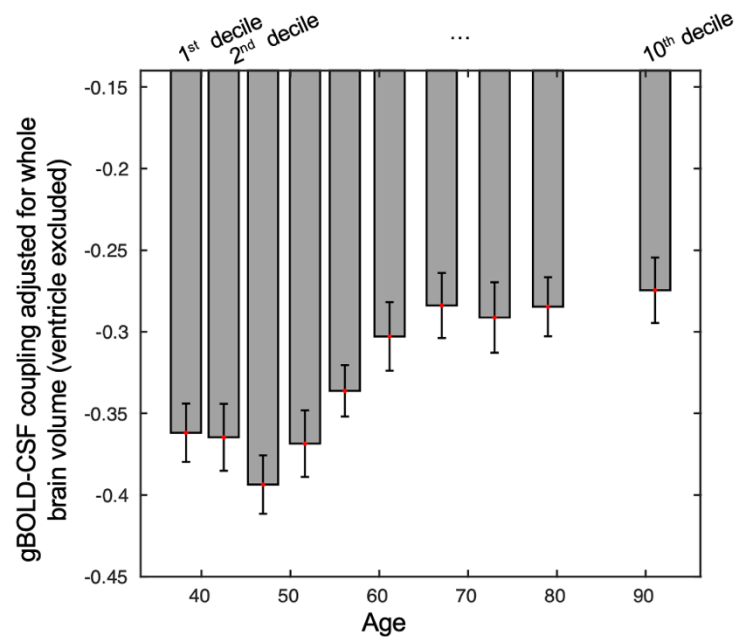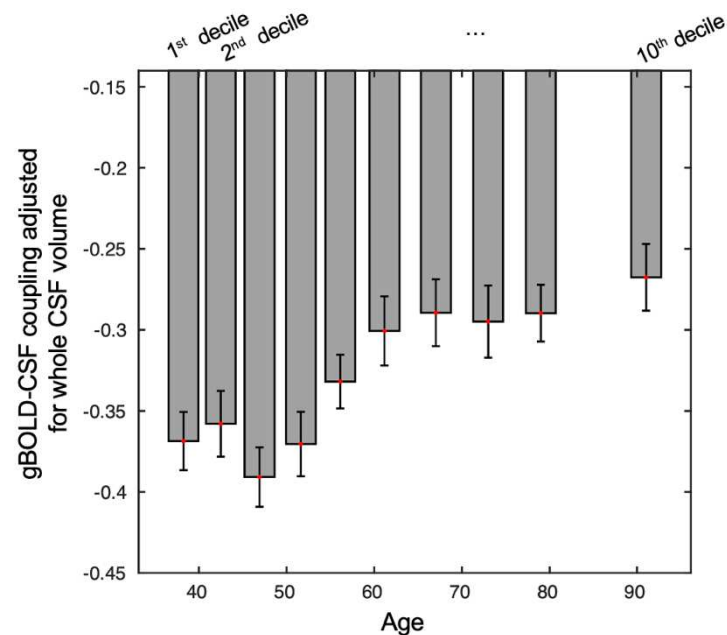
782

783

784

Fig. S3 The age-coupling association was not dominant by the whole brain volume. Consistent results as **Fig.1** were found when we regressed out the whole brain volume (ventricles excluded) from the gBOLD-CSF coupling for each rsfMRI session.

788

789

790

Fig. S4 The age-coupling association was not affected by the whole CSF volume. Similar results as **Fig.1** were found when the volume of the whole CSF area was regressed out from the gBOLD-CSF coupling for each rsfMRI session.